

Injected power control for grid-connected converter based on particle swarm optimization

Safa Sfoog Oleiwi, Abdulrahim Thiab Humod, Fadhil Abbas Hasan

Department of Electrical Engineering, University of Technology, Baghdad, Iraq

Article Info

Article history:

Received Jan 5, 2022

Revised Jun 13, 2022

Accepted Jul 13, 2022

Keywords:

Analysis of LCL filter

Distributed generation

Injected power control

LCL filter

Particle swarm optimization

ABSTRACT

Inductance–capacitance–inductance (LCL) filters are very attractive candidates for renewable energy system applications due to their high efficiency, high harmonic reduction, small bulk, and improved total harmonic distortion (THD). These papers take advantage of the capabilities of renewable energy sources and inject them into the network by using an inverter when it enters work at high loads at certain times. Therefore, it is necessary to control power with certain controllers. The proportional-integral controller (PI) is used; conventional methods for tuning the controller parameters cannot give satisfactory performance due to the high instability of the closed-loop system. This paper presents the particle swarm optimization (PSO) method for tuning the controller's parameters to achieve optimum performance associated with sufficient stability margin. The mathematical models for the LCL filter and the frequency response were investigated by using the bode-plot. The proposed approach shows effective results for both power control and harmonic reduction. The proposed PI-PSO controller gives overshoot (1.08%), settling time (0.03 sec), rise time (0.00035 sec) and improved THD from 10.29% to 1.67% with compared to using the trial-and-error method, which gives (1.035%), (0.015) and (0.003) and THD from 10.23% to 1.575%, respectively.

This is an open access article under the [CC BY-SA](https://creativecommons.org/licenses/by-sa/4.0/) license.



Corresponding Author:

Safa Sfoog Oleiwi

Department of Electrical Engineering, University of Technology

Alsinaa Street, Baghdad, Iraq

Email: eee.19.12@grad.uotechnology.edu.iq

1. INTRODUCTION

At current days distributed generations systems (DGs) have been used to generate electricity because of their high reliability and low gas emissions, especially for CO₂ gas, which made them environmentally friendly and low in pollution, and given the most important factor, which is cost, compared to the traditional source of electricity, it is more practical and less expensive, connected to DGs is a low voltage distribution tool for renewable power components which includes; Fuel cell, wind or photovoltaic, for the grid the usage of a power inverter [1]. DG units generate electricity closer to load centers, avoiding the expense of energy transportation and lowering transmission line power losses. Furthermore, when compared to centralized generation stations, DG solutions save more money [2]. As it is known that renewable energy sources generate direct current (DC) power, so it is necessary to use a power inverter to convert it into alternating current (AC) power, this is why it is used in these systems including active and reactive energy which can be controlled. However, in voltage source inverter (VSI), the pulse width modulation (PWM) approach causes the appearance of high and low harmonics, which are detrimental to the system's balance and must be eliminated [3]-[5]. That is why it's vital to utilize a filter to do away with these problems and treat them. In previous research, the inductor (L), inductor-capacitor (LC) and inductor-

capacitor-inductor (LCL)-filters are designed and they have the following characteristics. Despite its popularity and ease of use, a single inductor L-filter has a low attenuation and an excessive inductance rate. The voltage drop across the inductor causes negative machine dynamics, resulting in a long response time. The inverter switching frequency must have an excessive value to sufficiently attenuate the harmonics when using an L-filter [6]. L-type filters can attenuate -20 dB/dc, that's a small amount, so it needs a capacitor that produces a large and excessive impedance in the frequency variety. For modulations, the LC filter is ideal that have notably high load impedance and above running frequency. After that, it needs a large capacitance to reduce losses and thus cost. Nevertheless, this will also result in an increase in reactive power, In addition to the possibility of the appearance of the phenomenon of resonance [7]. Because it has a larger decoupling between the converter and the grid impedance, better attenuation of the switching frequency harmonics well as reducing total harmonics distortion (THD), to compensate for the high capacitance, the LCL-filter can be utilized. Since this system's stability will be affected by the filter's resonance, passive damping is utilized by connecting resistors in parallel with the filter output capacitors to damper the resonant harmonics [8].

This work proposed the power control by using PI controller, which has a fast response to changes in the control process since it takes instant corrective action when an error occurs, and it has a very stable control process if the proportional gain (Kp) and integral gain (Ki) factors (parameters of PI controller) are met and properly selected. The PI controller will be using two methods: the first is the traditional trial and error approach and the particle swarm optimization (PSO) algorithm. Power injection controlled with sudden or gradual load changes, through the usage of an LCL filter between the inverter and the grid, the harmonic is removed and the THD is reduced to less than 5%. The technique of decoupling control is employed. The important characteristic should be $i_q=0$, which gives the idea an easy configuration and secure manipulate [9].

This search was completed in the following sections: in section 2, the model of LCL-filter obtained between converter and network. The equations for the system is obtained by using the direct decoupling method. In section 3 show the transfer function of system with LCL filter, section 4 represent stability analysis of LCL filter, section 5 power control strategies and section 6 represents the simulation results for each controller PI, finally, the conclusions drawn from this work are summarized in section 7.

2. MATHEMATICAL MODEL OF LCL FILTER INVERTER

The network's stationary frame analysis can be expressed as shown in Figure 1 using Kirchhoff's voltage law, as shown in:

$$V_1 - r_1 i_1 - L_1 \frac{d}{dt} i_1 - V_c = 0 \quad (1)$$

$$V_1 - V_c = L_1 \frac{d}{dt} i_1 + r_1 i_1 \quad (2)$$

$$V_c - r_2 i_2 - L_2 \frac{d}{dt} i_2 - e = 0 \quad (3)$$

$$V_c - e = L_2 \frac{d}{dt} i_2 + r_2 i_2 \quad (4)$$

where: $i_1 = i_c + i_2$, $i_c = C \frac{d}{dt} V_c$, $L_2 = L_f + L_g$, $r_2 = r_f + r_g$

V_1 : The voltage of converter side.

i_1 : The current of converter side. L_f : The inductance of grid side filter.

V_c : The voltage of capacitance. L_g : The inductance of grid.

i_c : The current of capacitance. r_1 : The resistance of converter side filter.

i_2 : The current of grid. r_f : The resistance of grid side filter.

L_1 : The inductance of converter side filter. r_g : The resistance of grid.

The mathematical model inside the $\alpha\beta$ frame is:

$$V_{1\alpha\beta} - V_{c\alpha\beta} = r_1 i_{1\alpha\beta} + L_1 \frac{d}{dt} i_{1\alpha\beta} \quad (5)$$

$$V_{c\alpha\beta} - e_{\alpha\beta} = r_2 i_{2\alpha\beta} + L_2 \frac{d}{dt} i_{2\alpha\beta} \quad (6)$$

$$i_{c\alpha\beta} = C \frac{d}{dt} V_{c\alpha\beta} \quad (7)$$

$$i_{1\alpha\beta} = i_{c\alpha\beta} + i_{2\alpha\beta} \tag{8}$$

it is important to note that the two phase d-q system has a property, which is that any vector has an amount that rotates with the frame and with the same velocity, which is the angular velocity ω and the equations are as shown in:

$$V_{1d} - V_{cd} = r_1 i_{1d} + L_1 \frac{d}{dt} i_{1d} - L_1 \omega i_{1d} \tag{9}$$

$$V_{1q} - V_{cq} = r_1 i_{1q} + L_1 \frac{d}{dt} i_{1q} + L_1 \omega i_{1q} \tag{10}$$

$$V_{cd} - e_d = r_2 i_{2d} + L_2 \frac{d}{dt} i_{2d} - L_2 \omega i_{2d} \tag{11}$$

$$V_{cq} - e_q = r_2 i_{2q} + L_2 \frac{d}{dt} i_{2q} + L_2 \omega i_{2q} \tag{12}$$

where: $i_{cd} = C \frac{d}{dt} V_d$, $i_{cq} = C \frac{d}{dt} V_q$

The decoupling components are defined: $i_{1d}^{decoupled} = \omega L_1 i_{q1}$, $i_{q1}^{decoupled} = -\omega L_1 i_{d1}$. So the currents will be:

$$i_{1d} = i_{cd} + i_{2d} + \omega L_1 i_{q1} \tag{13}$$

$$i_{1q} = i_{cq} + i_{2q} - \omega L_1 i_{d1} \tag{14}$$

The three phase voltages and supply currents at the point of common coupling (PCC) are converted into their respective components using Clarke's transformation. The stationary components are later changed into their equivalent rotational d and q components, synchronized to the supply voltage, using Park's transformation [10]. The phase locked loop (PLL) will trace the phase angle difference between the inverter and grid voltages and set it to zero, as well as a current controller to control the inverter's signals and measure the voltage magnitude that must be synced [11]. The use of a stationary or rotating frame is a typical method of analyzing three-phase systems Figure 2.

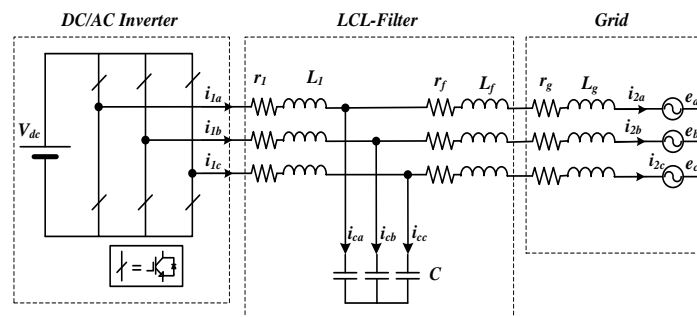


Figure 1. LCL-filter inverter connected to the grid

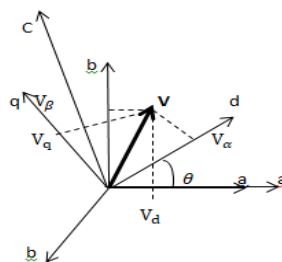


Figure 2. shows a stationary and a rotary dq frame

3. TRANSFER FUNCTION OF SYSTEM WITH LCL FILTER

Rearranging in (9) and (10) and putting S in place of:

$$\begin{aligned} \frac{d}{dt} V_{1dq} &= V_{cdq} + r_1 i_{1dq} + sL_1 i_{1dq} + L_1 \omega i_{1q} - L_1 \omega i_{1d} \\ V_{1dq} &= \frac{1}{sC} i_{cdq} + r_1 i_{1dq} + sL_1 i_{1dq} + L_1 \omega (i_{1q} - i_{1d}) \end{aligned} \quad (15)$$

where: $V_{cdq} = \frac{1}{sC} i_{cdq}$

$$i_{1dq} = i_{cdq} + i_{2dq} \quad (16)$$

In the same process, the carried out (11) and (12).

$$V_{cdq} - e_{dq} = r_2 i_{2dq} + sL_2 i_{2dq} + L_2 \omega (i_{2q} - i_{2d}) \quad (17)$$

$$e_{dq} = V_{cdq} - r_2 i_{2dq} - sL_2 i_{2dq} - L_2 \omega (i_{2q} - i_{2d})$$

$$e_{dq} = \frac{1}{sC} i_{cdq} - r_2 i_{2dq} - sL_2 i_{2dq} - L_2 \omega (i_{2q} - i_{2d}) \quad (18)$$

If the filter is perfect, harmonics higher than the fundamental harmonic do not appear in the LCL filter's output current ($e_{dq} = 0$) [8].

$$i_{cdq} = sCr_2 i_{2dq} + s^2 CL_2 i_{2dq} + sCL_2 \omega (i_{2q} - i_{2d}) \quad (19)$$

Substituting as shown in (16) and (19) in (15)

$$\begin{aligned} V_{1dq} &= \frac{1}{sC} [sCr_2 i_{2dq} + s^2 CL_2 i_{2dq} + sCL_2 \omega (i_{2q} - i_{2d})] + r_1 i_{cdq} + r_1 i_{2dq} + sL_1 i_{cdq} \\ &\quad + sL_1 i_{2dq} + L_1 \omega (i_{1q} - i_{1d}). \end{aligned}$$

$$\begin{aligned} V_{1dq} &= r_2 i_{2dq} + sL_2 i_{2dq} + L_2 \omega (i_{2q} - i_{2d}) + sCr_1 r_2 i_{2dq} + s^2 CL_2 r_1 i_{2dq} + sCL_2 r_1 \omega (i_{2q} - i_{2d}) + \\ &\quad r_1 i_{2dq} + s^2 L_1 Cr_2 i_{2dq} + s^3 CL_1 L_2 i_{2dq} + s^2 CL_1 L_2 \omega (i_{2q} - i_{2d}) + sL_1 i_{2dq} + L_1 \omega (i_{1q} - i_{1d}). \end{aligned}$$

$$\begin{aligned} V_{1dq} &= i_{2dq} [s^3 CL_1 - s^2 (CL_2 r_1 + CL_1 r_2 + CL_1 L_2 \omega (i_{2q} - i_{2d})) + \\ &\quad s (L_1 + L_2 + Cr_1 r_2 + CL_2 r_1 \omega (i_{2q} - i_{2d})) + (r_1 + r_2 + L_1 \omega (i_{1q} - i_{1d}))] \end{aligned} \quad (20)$$

For ($\omega = 0$) So the transfer function become: $\frac{i_{2dq}}{V_{1dq}} = \frac{1}{a_3 s^3 + a_2 s^2 + a_1 s + a_0}$, where: $a_0 = r_1 + r_2$, $a_1 = L_1 + L_2 + CL_1 L_2$, $a_2 = CL_2 r_1 + CL_1 r_2$, $a_3 = CL_1 L_2$

4. STEABILITY ANALYSIS OF LCL FILTER

To minimize resonance harmonics, the passive damping method has been used, which involves adding passive elements to the filter circuit, resistors in series or parallel with the capacitor are commonly used [12]-[16]. The serial branches minimize losses while lowering high-order harmonic dampening capacity. The parallel department, on the other hand, has no effect on low and excessive-order harmonics, but it does increase losses. The adding resistor, on the other hand, will result in higher loss and less attenuation of high-frequency harmonics. Alternatively, active damping strategies are used to suppress resonance and stabilize the system, with the basic idea being to introduce more variables as damping terms to the present control loop [17]-[20]. The frequency responses are investigated in Figure 3 by substituting the following values of inductances, capacitors, and resistances in transfer function. Where: $L_1 = 5.3052 \times 10^{-4} H$, $L_2 = 1.5321 \times 10^{-4} H$, $C = 1.10022 \times 10^{-4} F$.

Figure 3(a) shows the frequency response of closed-loop system when neglecting parasitic resistance of the filter inductance (i.e. $r_1, r_2 = 0$), while Figure 3(b) shows the frequency response of the actual inductance resistance $r_1 = 0.1667 \Omega$, $r_2 = 0.0096 \Omega$. It's noted from Figure 3 that when a certain value of resistors is added to the filter, the system becomes more stable than the purely inductive filter.

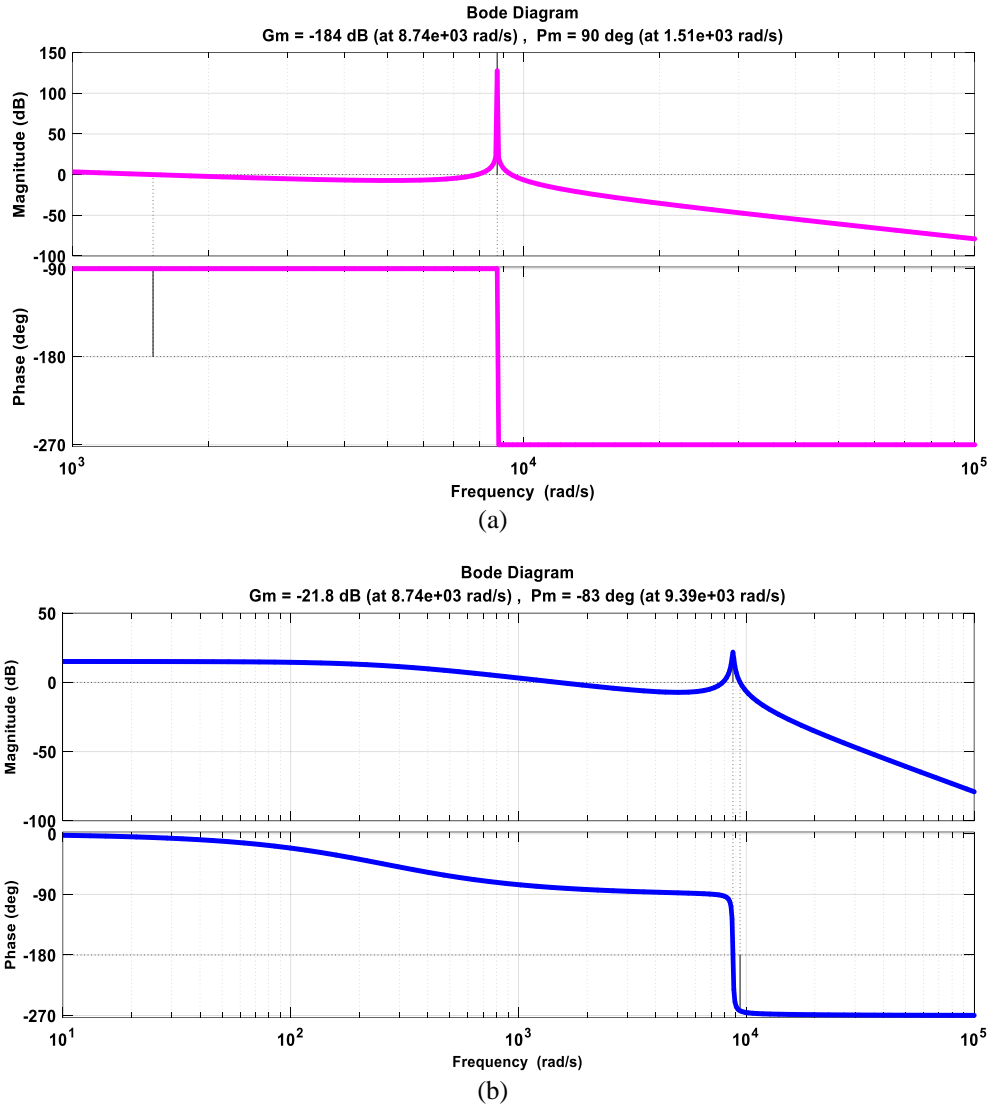


Figure 3. The frequency response of the LCL-filter for, (a) $r_1, r_2 = 0$ and (b) $r_1 = 0.1667 \Omega, r_2 = 0.0096 \Omega$

5. POWER CONTROL STRATEGIES

Controlling the active and reactive components of the source through implementing control strategies on the inverter could be used to achieve power and voltage regulation techniques [21]-[25]. Grid converter power control is based on instantaneous power theory and, as a result, on a reference frame definition of power. The VOC is based on the rotation of a dq frame at a high speed with the d axis aligned with the grid voltage vector. The current i_d^* is controlled to injected active power and i_q^* is controlled the reactive power. For making the grid current vector to be in phase with the grid voltage vector, i_q^* should be zero [8]. As a result, the grid converter's active and reactive power are shown in:

$$P = \frac{3}{2} e_d i_d + e_q i_q \tag{21}$$

$$Q = \frac{3}{2} e_q i_d - e_d i_q \tag{22}$$

where:

P: Real active power, Q: Real reactive power

Active and reactive power will be proportional to i_d and i_q , respectively, supposing the d axis is correctly aligned with the grid voltage $e_q = 0$. The block diagram of the power control system is shown in Figure 4.

$$P = \frac{3}{2} e_d i_d \tag{23}$$

$$Q = \frac{-3}{2} e_d i_q \tag{24}$$

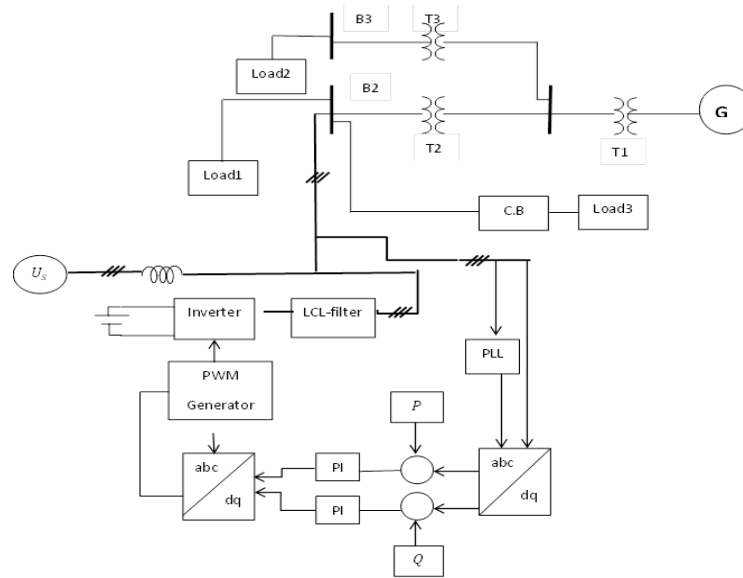


Figure 4. The control system's structure diagram

5.1. PQ open-loop control

Powers feed-forward control is the most straightforward ways to implement voltage-oriented control. The active and reactive power command signals are then translated into the reference current's d and q components using the matrix in:

$$\begin{bmatrix} i_d^* \\ i_q^* \end{bmatrix} = \frac{1}{V_{gd}^2 + V_{gq}^2} \begin{bmatrix} V_{gd} & -V_{gq} \\ V_{gq} & V_{gd} \end{bmatrix} \begin{bmatrix} P^* \\ Q^* \end{bmatrix} \tag{25}$$

where:

V_{gd} : Grid d-axis voltage, V_{gq} : Grid q-axis voltage

i_d^* : d- axis required current, i_q^* : q- axis required current, P^* : Injected active power,

Q^* : Injected reactive power

5.2. PQ closed-loop control

The dynamics of powers control can be determined as a result of changes in grid voltage using closed-loop control:

$$i_d^* = P^* - P \tag{26}$$

$$i_q^* = Q^* - Q \tag{27}$$

where: $P = V_{gd}i_{gd} + V_{gq}i_{gq}$, $Q = -V_{gq}i_d + V_{gd}i_q$.

6. SIMULATION AND RESULTS

6.1. PI controller with trial-and-error method

To optimize the PI controller gain, many common tuning methods have been utilized, such as trial and error tuning methods to obtain optimal values for the PI controller values K_p and K_i . The PI controller was used to control the injection of the required power into this network, which is a generator that generates electrical energy and feeds three different loads that enter the work at certain times. This means that the

network generator will need to prepare a higher capacity in the event of high loads entering the work. The power from the renewable energy source will be injected into it to help it equip the required energy with the overall. System simulation shown in Figure 5. Table 1 shows how PI controller gains are chosen by trial and error.

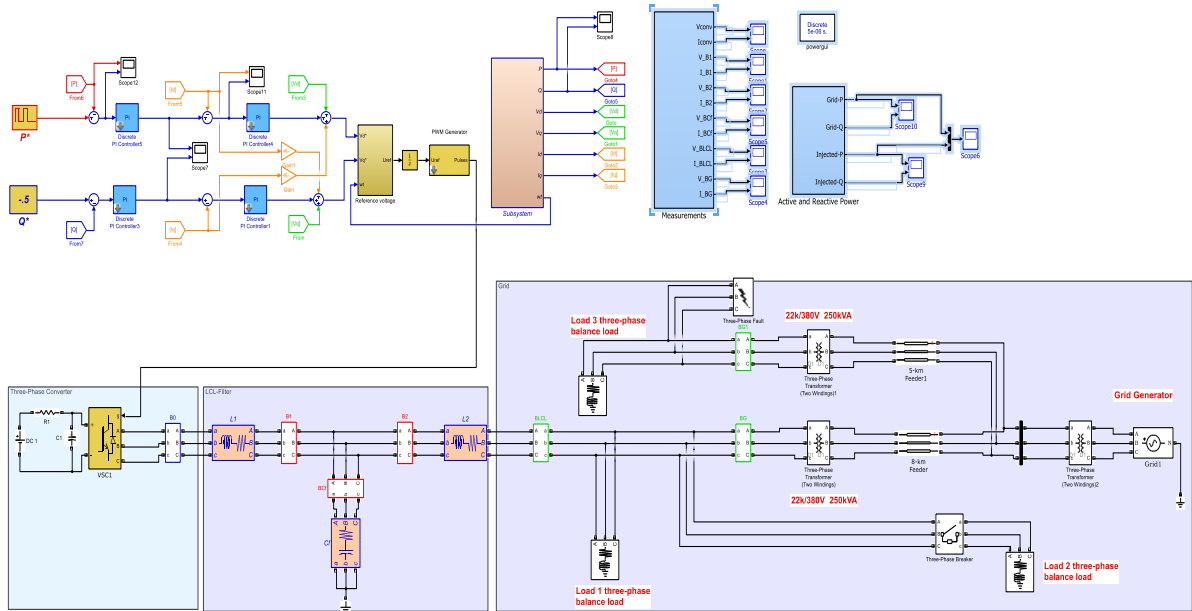


Figure 5. Simulation model of power control with LCL-filter grid-connected converter

Table 1. The Kp and Ki values

Controller	Kp	Ki
Active power controller	10	500
Id controller	0.1	50

Figure 6 depicts a comparing simulation results in Figure 6(a) the grid and injected active power, it was observed the times when the loads enter the work and how the grid is prepared for them, but at the time of the need to inject power. While, Figure 6(b) shows the injected active power and the performance of the controller was excellent and it gave the parameters: overshoot=1.08%, settling time 0.03 sec, rise time=0.00035 sec. Figure 7 comparing simulation results in Figure 7(a) it shows the grid's reactive power and the injected reactive power Figure 7(b), as there is no power injection in this work and its value is zero. Figure 8 shows the simulation results of the dq-axis current control with PI controller with trial-and-error method Figure 8(a) the d-axis control current and Figure 8(b) the q-axis current control.

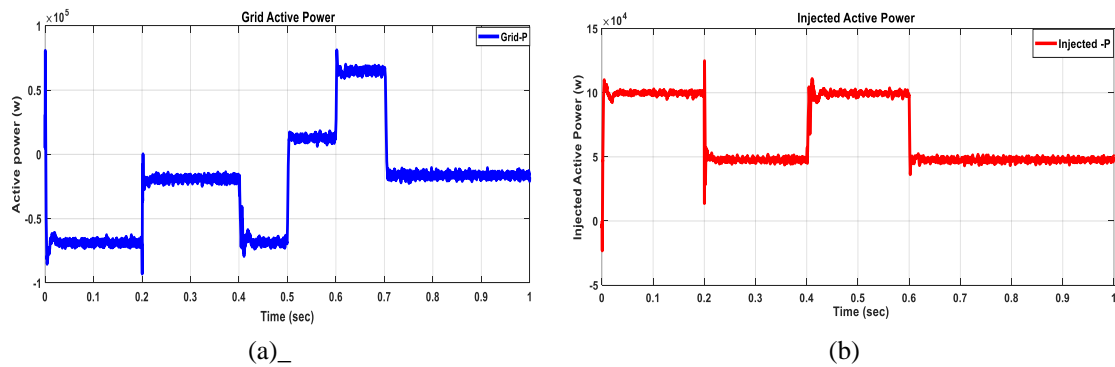


Figure 6. System active power, (a) grid active power and (b) the injected active power

The current on the d-axis (i_d) is what affects the injected effective power (P), and also the q-axis current (i_q) for injected reactive power (Q). Therefore, controlling the current is controlling the power, and this form is identical. So controlling current is controlling power. Figure 9 shows the currents after using the PI controller with trial and error method and how the current increases during the period of increasing high loads and decreases during the period when the loads are out of work which Figure 9(a) the filter current and Figure 9(b) the grid current.

By analyzing the harmonic of the converter current and the filter current, it was detected that the improvement of the voltage is obviously noticeable, as the voltage drop has become much lower, furthermore to eliminating high harmonics and keeping the necessary fundamental harmonic. THD was reduced from 10.29% to 1.67% and this last rate is permissible according to IEEE 929-2000 and IEEE 519-1992 specifications, as THD is less than 5% as presented in Figure 10, where Figure 10(a) presents the THD of the converter current, and Figure 10(b) depicts the LCL filter current.

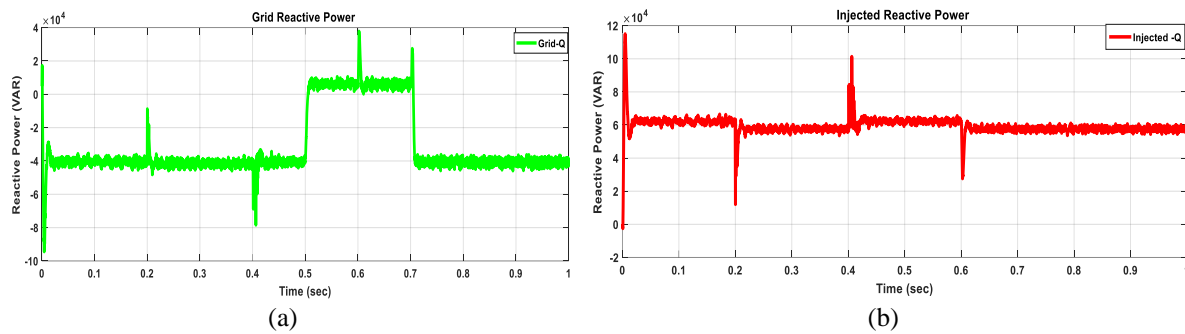


Figure 7. System reactive power, (a) grid reactive power and (b) the injected reactive power

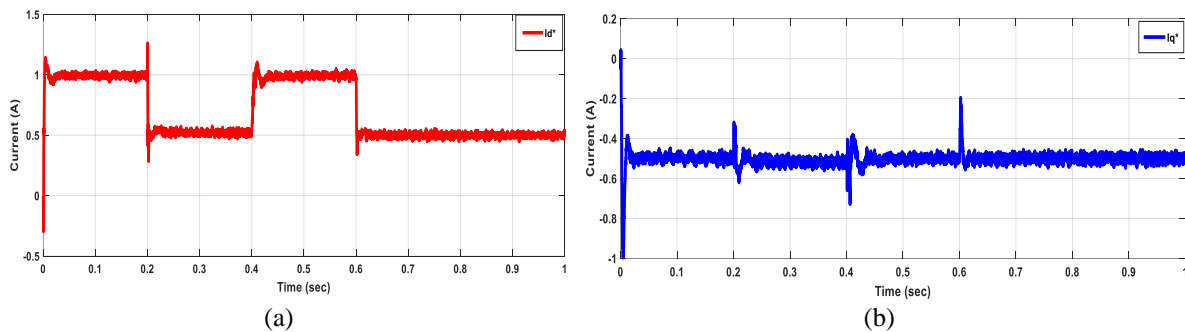


Figure 8. Simulation results of the dq-axis current control with PI controller with trial-and-error (a) D- axis required current and (b) Q-axis required current

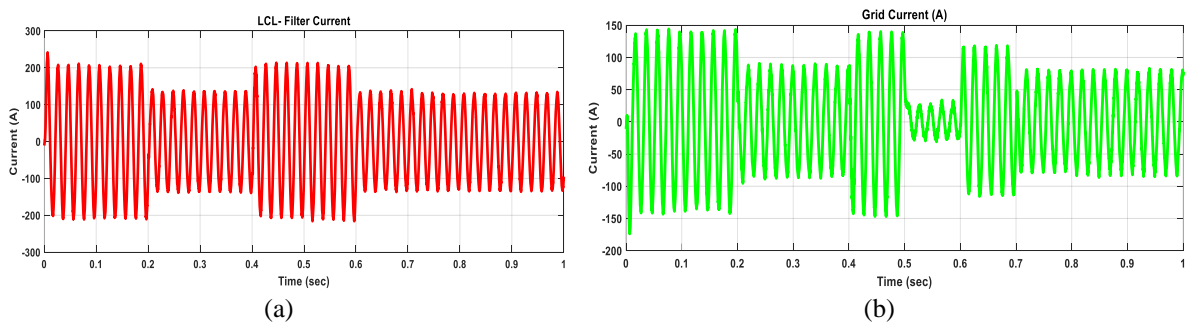


Figure 9. Currents after using the PI controller with trial and error (a) LCL-filter current and (b) grid current

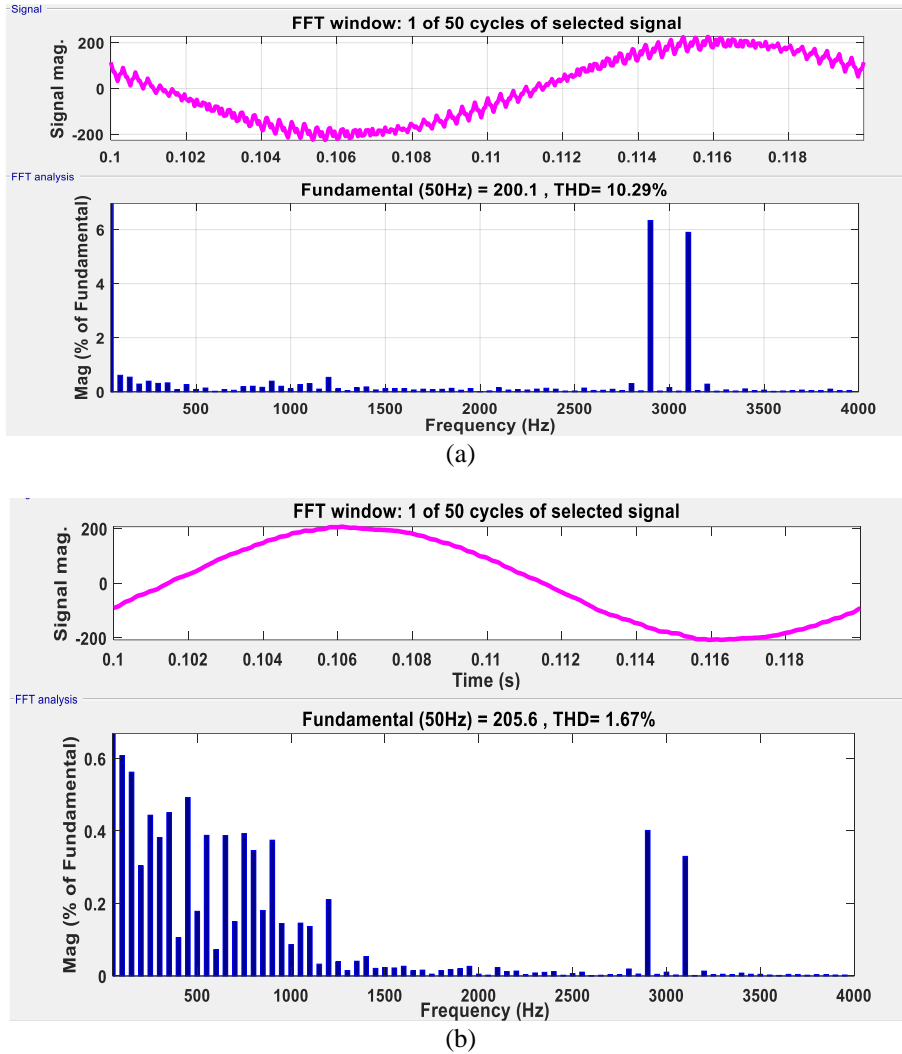


Figure 10. The THD, (a) Converter current and (b) LCL filter current

6.2. PI-PSO controller with multi-objectives fitness function

Then several intelligent technologies, such as PSO technology, have been presented to increase the capabilities of classical PI parameter tuning procedures in order to improve PI tuning. ITSE is the PSO objective function employed in this study. ITSE is expressed by the components integrator, product, clock, math function and work space blocks. To determine the best controller parameters, the PSO method employs sub-M-file programs. The following factors are used in the optimization method where C1, C2 equal to (1.3), W is (0.9), number of iterations is (100) and number of particles is (30). Table 2 shows the obtained parameters of the tow PI controllers. The tendency of particles moving within the searching field to the global optimal solution is depicted in Figure 11, which tracks the corresponding particles of the global optimal solution (the shown particles are part of the total particles).

Table 2. Optimum controller parameters

Controller	Kp	Ki	Fitness
Active power controller	7.45	735.64	63.22
Id controller	0.3305	55.8527	

Figure 12 shows the controller performance, in Figure 12(a) the injected active power is depicted, Figure 12(b) shows the infected reactive power. Obviously, it performed admirably and provided the following parameters: overshoot=1.035%, settling time=0.015 sec, rise time=0.003 sec. This is an excellent result for a steady state error, but the overshoot is somewhat high. Figure 13 shows the simulation results of the dq-axis current control with PI-PSO controller with multi-objectives fitness function Figure 13(a) the d-

axis control current and Figure 13(b) the q-axis current control. Figure 14 shows a total harmonic distortion; Figure 14(a) shows the converter current THD, and Figure 14(b) shows the LCL filter current THD. These show that the THD was reduced from 10.23% to 1.57%. Finally, Figure 15 illustrates a performance comparison between the proposed controller and the traditional controller.

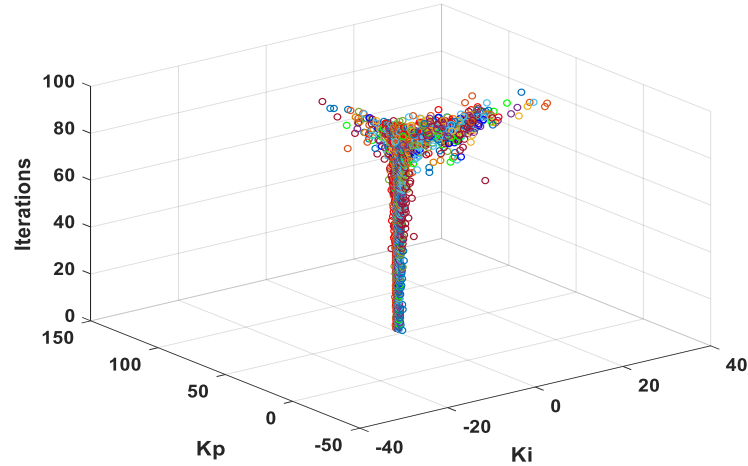


Figure 11. Particles tend to converge on the global optimum

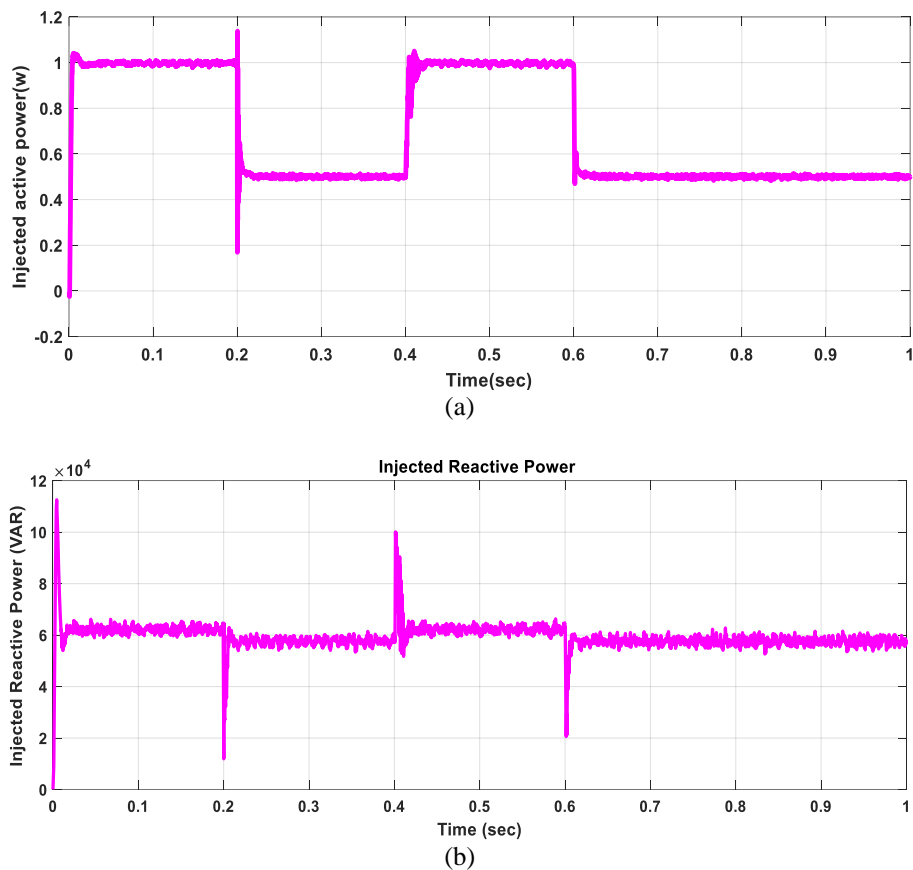


Figure 12. Controller performance (a) injected active current and (b) the injected reactive power

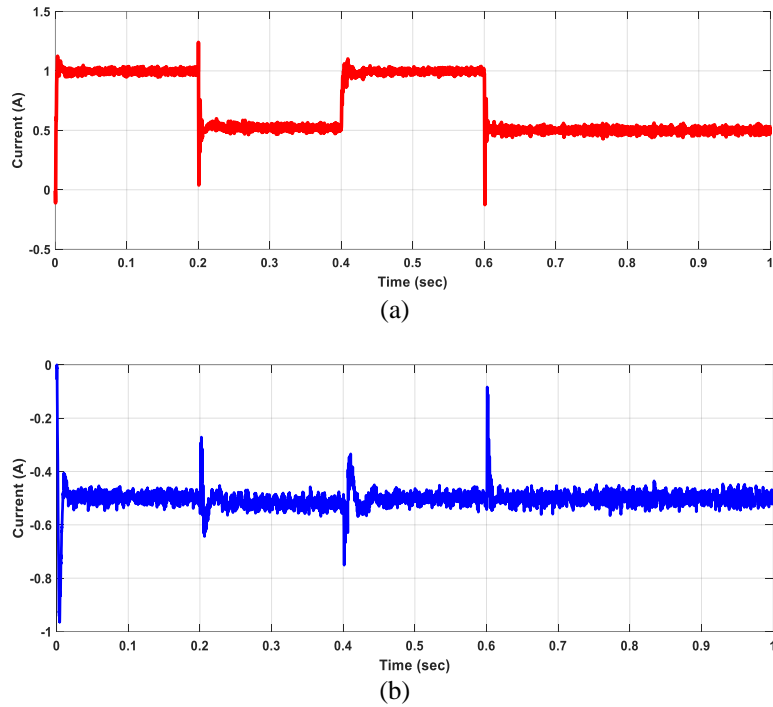


Figure 13. Simulation results of the dq-axis current control with PI-PSO controller (a) D-axis control current and (b) Q-axis control current

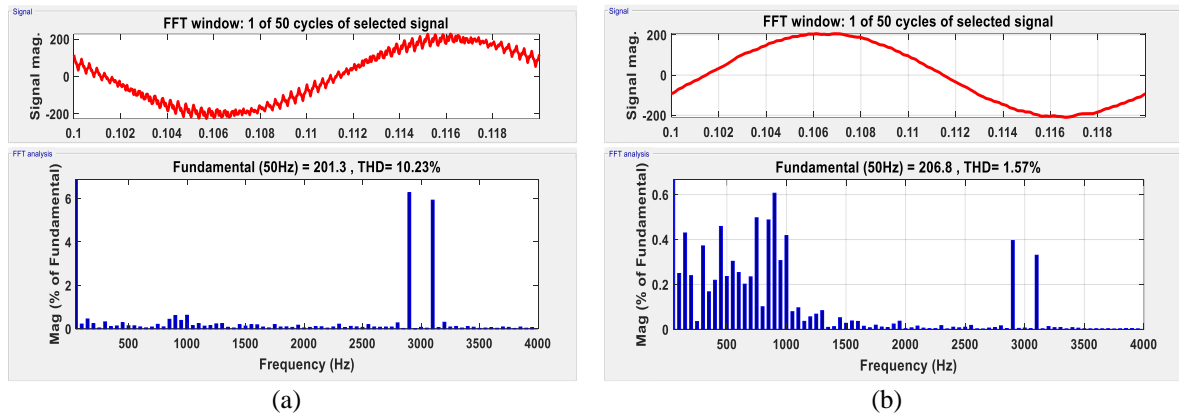


Figure 14. The injected current THD (a) converter current and (b) LCL filter current

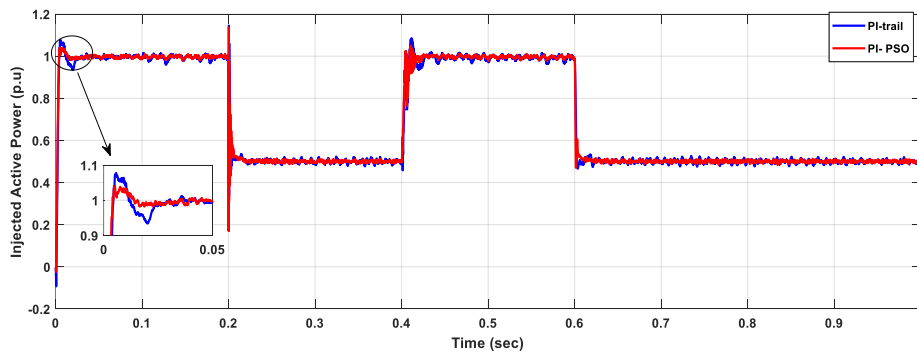


Figure 15. Performance comparison of the injected active power between the proposed and the traditional controllers

7. CONCLUSION

LCL filter is selected for usage in renewable energies applications, because of its high features. PI controller with trial-and-error method give 1.08%, 0.03 sec and 0.00035 sec for overshoot, settling time, rise time respectively and improving THD from 10.29% to 1.67% and PI-PSO controller with ITSE objective function give (63.2203996), (1.035%), (0.015) sec, (0.003) sec and from 10.23% to 1.57% for overshoot, settling time, rise time and improving THD respectively ,very exceptional in filtering from unwelcome harmonics and reducing the THD to less than 5%, according to the international standard for IEEE 929-2000 and IEEE 519-1992, in addition to that it is light in weight and low in cost compared to other types. Depending on the results obtained by working in this paper the PI controller results are great especially in linear applications. Since the control of injected power tight and balanced, it does not change as demined even after operating the load in the grid.

REFERENCES

- [1] Y. He, H. S. H. Chung, C. T. Lai, X. Zhang, and W. Wu, "Active cancelation of equivalent grid impedance for improving stability and injected power quality of grid-connected inverter under variable grid condition," *IEEE Transactions on Power Electronics*, vol. 33, no. 11, pp. 9387–9398, Nov. 2018, doi: 10.1109/TPEL.2018.2793459.
- [2] E. Karunarathne, J. Pasupuleti, J. Ekanayake, and D. Almeida, "Network loss reduction and voltage improvement by optimal placement and sizing of distributed generators with active and reactive power injection using fine-tuned PSO," *Indonesian Journal of Electrical Engineering and Computer Science*, vol. 21, no. 2, pp. 647–656, Feb. 2020, doi: 10.11591/ijeecs.v21.i2.pp647-656.
- [3] J. Xu, T. Tang, and S. Xie, "Research on low-order current harmonics rejections for grid-connected LCL-filtered inverters," *IET Power Electronics*, vol. 7, no. 5, pp. 1227–1234, May 2014, doi: 10.1049/iet-pel.2013.0477.
- [4] W. Choi, W. Lee, D. Han, and B. Sarlioglu, "New configuration of multifunctional grid-connected inverter to improve both current-based and voltage-based power quality," *IEEE Transactions on Industry Applications*, vol. 54, no. 6, pp. 6374–6382, Nov. 2018, doi: 10.1109/TIA.2018.2861737.
- [5] Y. Gui, Q. Xu, F. Blaabjerg, and H. Gong, "Sliding mode control with grid voltage modulated DPC for voltage source inverters under distorted grid voltage," *CPSS Transactions on Power Electronics and Applications*, vol. 4, no. 3, pp. 244–254, Sep. 2019, doi: 10.24295/CPSSPEA.2019.00023.
- [6] M. El-Habrouk, M. K. Darwish, and P. Mehta, "Active power filters: A review," *IEE Proceedings - Electric Power Applications*, vol. 147, no. 5, p. 403, 2000, doi: 10.1049/ip-epa:20000522.
- [7] H. Akagi, "Active harmonic filters," *Proceedings of the IEEE*, vol. 93, no. 12, pp. 2128–2141, Dec. 2005, doi: 10.1109/JPROC.2005.859603.
- [8] H. Goh, M. Armstrong, and B. Zahawi, "Adaptive control technique for suppression of resonance in grid-connected PV inverters," *IET Power Electronics*, vol. 12, no. 6, pp. 1479–1486, May 2019, doi: 10.1049/iet-pel.2018.5170.
- [9] R. Teodorescu, M. Liserre, and P. Rodríguez, *Grid Converters for Photovoltaic and Wind Power Systems*. Wiley, 2011.
- [10] User Guide, "Park, inverse park and clarke, inverse clarke software, transformations MSS Implementation," *Microsemi*, 2013. [Online]. Available: https://www.microsemi.com/document-portal/doc_view/132799-park-inverse-park-and-clarke-inverse-clarke-transformations-mss-software-implementation-user-guide.
- [11] S. Gorai, D. Sattianadan, V. Shanmugasundaram, S. Vidyasagar, G. P. Kumar, and M. Sudhakaran, "Investigation of voltage regulation in grid-connected PV system," *Indonesian Journal of Electrical Engineering and Computer Science*, vol. 19, no. 3, p. 1131, Sep. 2020, doi: 10.11591/ijeecs.v19.i3.pp1131-1139.
- [12] M. Malinowski and S. Bernet, "A simple voltage sensorless active damping scheme for three-phase PWM converters with an LCL filter," *IEEE Transactions on Industrial Electronics*, vol. 55, no. 4, pp. 1876–1880, Apr. 2008, doi: 10.1109/TIE.2008.917066.
- [13] M. Prodanović and T. C. Green, "Control and filter design of three-phase inverters for high power quality grid connection," *IEEE Transactions on Power Electronics*, vol. 18, no. 1 II, pp. 373–380, Jan. 2003, doi: 10.1109/TPEL.2002.807166.
- [14] I. J. Gabe, V. F. Montagner, and H. Pinheiro, "Design and implementation of a robust current controller for VSI connected to the grid through an LCL filter," *IEEE Transactions on Power Electronics*, vol. 24, no. 6, pp. 1444–1452, Jun. 2009, doi: 10.1109/TPEL.2009.2016097.
- [15] G. Shen, D. Xu, L. Cao, and X. Zhu, "An improved control strategy for grid-connected voltage source inverters with an LCL filter," *IEEE Transactions on Power Electronics*, vol. 23, no. 4, pp. 1899–1906, Jul. 2008, doi: 10.1109/TPEL.2008.924602.
- [16] E. Twining and D. G. Holmes, "Grid current regulation of a three-phase voltage source inverter with an LCL input filter," *IEEE Transactions on Power Electronics*, vol. 18, no. 3, pp. 888–895, May 2003, doi: 10.1109/TPEL.2003.810838.
- [17] F. Liu, Y. Zhou, S. Duan, J. Yin, B. Liu, and F. Liu, "Parameter design of a two-current-loop controller used in a grid-connected inverter system with LCL filter," *IEEE Transactions on Industrial Electronics*, vol. 56, no. 11, pp. 4483–4491, Nov. 2009, doi: 10.1109/TIE.2009.2021175.
- [18] X. Wang, X. Ruan, S. Liu, and C. K. Tse, "Full feedforward of grid voltage for grid-connected inverter with LCL filter to suppress current distortion due to grid voltage harmonics," *IEEE Transactions on Power Electronics*, vol. 25, no. 12, pp. 3119–3127, Dec. 2010, doi: 10.1109/TPEL.2010.2077312.
- [19] F. A. Magueed and J. Svensson, "Control of VSC connected to the grid through LCL-filter to achieve balanced currents," in *Conference Record - IAS Annual Meeting (IEEE Industry Applications Society)*, 2005, vol. 1, pp. 572–578, doi: 10.1109/IAS.2005.1518364.
- [20] E. Wu and P. W. Lehn, "Digital current control of a voltage source converter with active damping of LCL resonance," in *Conference Proceedings - IEEE Applied Power Electronics Conference and Exposition - APEC*, 2005, vol. 3, pp. 1642–1649, doi: 10.1109/APEC.2005.1453259.
- [21] J. Dannehl, F. W. Fuchs, and P. B. Thøgersen, "PI state space current control of grid-connected PWM converters with LCL filters," *IEEE Transactions on Power Electronics*, vol. 25, no. 9, pp. 2320–2330, Sep. 2010, doi: 10.1109/TPEL.2010.2047408.
- [22] Y. Gui, C. Kim, C. C. Chung, J. M. Guerrero, Y. Guan, and J. C. Vasquez, "Improved direct power control for grid-connected voltage source converters," *IEEE Transactions on Industrial Electronics*, vol. 65, no. 10, pp. 8041–8051, Oct. 2018, doi: 10.1109/TIE.2018.2801835.

- [23] A. S. Al-Ogaili *et al.*, "A three-level universal electric vehicle charger based on voltage-oriented control and pulse-width modulation," *Energies*, vol. 12, no. 12, p. 2375, Jun. 2019, doi: 10.3390/en12122375.
- [24] M. F. Yaakub, M. A. M. Radzi, M. Azri, and F. H. M. Noh, "LCL filter design for grid-connected single-phase flyback microinverter: A step by step guide," *International Journal of Power Electronics and Drive Systems (IJPEDS)*, vol. 12, no. 3, pp. 1632–1643, Sep. 2021, doi: 10.11591/ijpeds.v12.i3.pp1632-1643.
- [25] G. Tahri, Z. A. Foithi, and A. Tahri, "Fuzzy logic control of active and reactive power for a grid-connected photovoltaic system using a three-level neutral-point-clamped inverter," *International Journal of Power Electronics and Drive Systems (IJPEDS)*, vol. 12, no. 1, p. 453, Mar. 2021, doi: 10.11591/ijpeds.v12.i1.pp453-462.

BIOGRAPHIES OF AUTHORS



Safa Sfoog Oleiwi    was born in Baghdad, Iraq in 1994. She received a bachelor's degree in electrical engineering from University of Technology, Iraq in 2015. She is currently studying toward a Master's degree of science in electrical power engineering at the University of Technology, Iraq. She can be contacted at email: eee.19.12@grad.uotechnology.edu.iq.



Prof. Dr. Abdulrahim Thiab Humod    He received his B.Sc. in the Department of Electrical and Electronic Engineering, Military engineering college, Iraq, respectively in 1984. He received his M.Sc in 1990 (control and guidance) from the Military engineering college, Iraq. His Ph.D. from Military engineering college (control and guidance) He is now a Professor in University of Technology, Iraq. He research interests are control and guidance. He can be contacted at email: 30040@uotechnology.edu.iq.



Asst. Prof. Dr. Fadhil Abbas Hasan    was born in Baghdad, Iraq in February 17, 1970. He received the B.Sc. from the university of Al-Mustansiryah, Baghdad, Iraq, in 1991, in electrical engineering. And he received the M.Sc. and Ph.D. degrees from University of Technology, in 2008 and 2017 respectively, in electrical machine and control engineering. In 2008, he joined the department of electrical engineering at university of technology, Baghdad, in Iraq, as an asst. lecturer. Currently he is an Asst. Prof. in the department of electrical engineering at University of Technology, Baghdad, in Iraq. He has published over 22 refereed journal and conference papers in the areas of induction heating, control systems, power electronics and electrical machines. He can be contacted at email: 30077@uotechnology.edu.iq.